Thermoelectric power of overdoped Tl2201 crystals: charge density waves and T^1 and T^2 resistivities

OPEN ACCESS
IOP Publishing
Superconductor Science and Technology
Supercond. Sci. Technol. **37** (2024) 015017 (8pp)
https://doi.org/10.1088/1361-6668/ad1463

Thermoelectric power of overdoped Tl2201 crystals: charge density waves and T^1 and T^2 resistivities

J R Cooper[1,*], J C Baglo[2,*], C Putzke[3,5] and A Carrington[4]

[1] Cavendish Laboratory, University of Cambridge, J. J. Thomson Avenue, Cambridge CB3 0HE, United Kingdom
[2] Département de physique and Institut quantique, Université de Sherbrooke, Sherbrooke, Québec, Canada
[3] Institute of Materials, École Polytechnique Fédéral de Lausanne, Lausanne, Switzerland
[4] H. H. Wills Physics Laboratory, University of Bristol, Bristol BS8 1TL, United Kingdom

E-mail: jrc19@cam.ac.uk and Jordan.Baglo@USherbrooke.ca

Received 10 April 2023, revised 23 November 2023
Accepted for publication 11 December 2023
Published 19 December 2023

Abstract

We report measurements of the in-plane thermoelectric power (TEP) for an overdoped (OD) crystal of the single layer cuprate superconductor $Tl_2Ba_2CuO_{6+x}$ (Tl2201) at several hole concentrations (p), from 300 or 400 K to below the superconducting transition temperature (T_c). For $p = 0.192$ and 0.220, small upturns in the TEP below 150 K are attributed to the presence of charge density waves (CDW) detected by resonant inelastic x-ray scattering studies. This suggests that measurement of the TEP could provide a simple and effective guide to the presence of a CDW. Over a certain temperature range, often strongly restricted by the CDW, the TEP is consistent with the Nordheim-Gorter rule and the T^1 and T^2 terms in the in-plane resistivity of similar crystals observed below 160 K. Two scenarios in which the T^1 scattering term is uniform or non-uniform around the Fermi surface are discussed. As found previously by others, for uniform scattering the T^1 terms give scattering rates (τ^{-1}) at lower p that are somewhat larger than the Planckian value $k_BT/\hbar$ and fall to zero for heavily OD crystals. Near 160 K, τ^{-1} from the T^2 terms corresponds to the Planckian value.

Supplementary material for this article is available online

Keywords: cuprates, thermoelectric power, charge density waves, electrical resistivity

1. Introduction

Identifying the pairing mechanism in cuprate superconductors and the origin of the characteristic T-linear behavior of the in-plane electrical resistivity, are still controversial and unsolved questions that may turn out to be closely related. In this regard single crystals of $Tl_2Ba_2CuO_{6+x}$ (Tl2201) are of great interest because their superconducting transition temperature (T_c) can be progressively reduced from 90 K to zero by increasing the oxygen content, x, and they have lower in-plane residual resistivity than other cuprates such as $La_{2-x}Sr_xCuO_4$ (LSCO) and $Bi_2Sr_2CuO_{6+\delta}$ that can be overdoped (OD). Furthermore, any van Hove singularity is well away from the Fermi energy [1]. Quantum oscillation (QO) experiments, e.g. [2] show that heavily OD crystals with $T_c \leqslant 26$ K have a large Fermi surface. There appears to be no work on strongly underdoped (UD) Tl2201 crystals, with difficulties caused, at least partly, by the volatility and toxicity of thallium compounds, but this does not affect our conclusions. Recently,

[5] Present address: Max-Planck-Institute for the Structure and Dynamics of Matter, Luruper Chaussee 149, Geb. 99 (CFEL), 22761 Hamburg, Germany.
[*] Authors to whom any correspondence should be addressed.

charge density waves (CDW) have been detected below 150 K in a resonant inelastic x-ray scattering (RIXS) study of OD Tl2201 crystals [3] with higher T_c. The question as to whether this can account for the unusual evolution of the Hall number as the hole doping (p) is reduced [1] is still being debated [4]. In this paper we report measurements of the in-plane thermoelectric power (TEP), $S_a(T)$ for a single crystal from the same preparation batch (October 2014) as in the RIXS and Hall effect work. We argue that the CDW gives a small but distinct upturn in $S_a(T)$ below 150 K. This conclusion is reinforced by the observation of similar upturns in all polycrystalline samples [5] with $T_c \geqslant 29$ K. Such data usually agree reasonably well with measurements of $S_a(T)$ on single crystals.

We discuss in-plane electrical resistivity $\rho_a(T)$ data [1] for Tl2201 crystals and show that the TEP is consistent with the T^1 and T^2 terms in $\rho_a(T)$ observed below 160 K and the Nordheim-Gorter (NG) rule. Corresponding scattering rates τ^{-1} are compared with the Planckian rate $k_BT/\hbar$ [6–8]. We estimate τ^{-1} at low T from $\rho_a(0)$ and raise the question as to whether the residual low-T specific heat of OD Tl2201 [9] is caused by standard pair-breaking in a d-wave superconductor [10, 11] combined with a decrease in the strength of the pairing interaction [12, 13], or whether it is caused by the pairing interaction $V_{kk'}$ being sufficiently anisotropic so that some electrons are not paired. Namely if the T^1 scattering term is much weaker on some parts of the Fermi surface does this imply that $V_{kk'}$ is much smaller there?

2. Results and analysis

2.1. Effect of CDW on the TEP

Above 1.1 T_c the TEP of OD cuprates generally varies approximately as $a + b(T/300)$, where $a \simeq 1$ to 2 μV K^{-1} and b changes from $\simeq -1$ to -10 μV K^{-1} as p is increased from 0.16, the value for maximum T_c, to the upper edge of the superconducting dome [5] while for UD samples it is usually positive and much larger [5]. TEP data were taken in an earlier, independent research project before the RIXS studies, using the method described in the appendix. One crystal was used for the TEP work and re-annealed to give successive T_c values of 26.5 K, 29 K, 67 K and 88 K, annealing conditions are given as supplementary information [14]. A small correction $\simeq +0.1\mu$V K^{-1} below 50 K has been made for the $T_c =$ 29 K and 26.5 K data using the phosphor bronze results shown in the appendix. AC susceptibility data for various crystals of Tl2201 with small AC fields parallel and perpendicular to the CuO_2 layers after different annealing treatments are reported as supplementary information [14]. They reveal an unexpectedly complex behavior and give evidence for two oxygen diffusion processes with very different time scales. It is probable that one or both of these are influenced by the concentration of Cu ions on Tl sites. This data could be useful for future studies. TEP data for polycrystalline samples [5] with $T_c = 84$ K, 82 K, 59 K, 29 K and less than 4 K, provide important confirmation of the present work.

Figure 1(a) shows that the in-plane TEP $S_a(T)$ for the same Tl2201 crystal with T_c values of 88 K and 67 K has a small upturn below ∼150 K, where there is also a clear change in the derivative dS_a/dT, as shown in figure 1(b), but there is no such effect for $T_c = 26.5$ K. For $T_c = 29$ K there is marginal evidence for a CDW with an onset near 40 K as indicated in figure 3. All this correlates well with RIXS measurements on Tl2201 crystals from the same preparation batch for which CDWs were detected for T_c values of 56 K and 45 K but not for 22 K [3]. TEP data for $T_c = 88$ K, on an expanded scale in figure 1(c), show a particularly clear anomaly near 145 K. The CDW onset temperature for $T_c = 45$ K is 150 K as shown by the RIXS data on the right hand scale of figure 1(b) but unfortunately the onset temperature of 160 K shown in [3] for $T_c = 56$ K is only an upper bound. Although better overlap of T_c values would have been desirable it is very probable that the changes in $S_a(T)$ and dS_a/dT near 150 K shown in figures 1(a)–(c) as well as at various temperatures for the polycrystalline data in [5] are caused by a CDW. This agreement is potentially useful because it shows that the TEP is a sensitive probe of the CDW and could be used to study its pressure dependence and possibly its magnetic-field dependence. Data for the OD88 crystal and the OD84 polycrystalline sample [5] show that the CDW is still present at lower p, which is a new finding.

2.2. T^1 and T^2 terms in the resistivity

Resistivity data [1] for five different crystals from the same preparation batch are shown in figure 2(a). As noted in [3] there appears to be no effect of the CDW on the in-plane resistivity $\rho_a(T)$. This is unusual since other CDW materials do show resistivity anomalies, but it is reinforced by the derivative plots in figure 2(b). Although there is a change in slope of $d\rho_a(T)/dT$ near 160 K, we do not believe that this is caused by a CDW. It is also present for the crystal with $T_c = 26.5$ K and a crystal from another batch with $T_c = 17$ K as well as for older data scanned in from [15].

Such derivative plots [16, 17] are a convenient way of applying the formula

$$\rho_a(T) = \alpha_0 + \alpha_1 T + \alpha_2 T^2 \qquad (1)$$

because the range of fit is easily seen by inspection. They suggest that there are two distinct values for the T^1 and T^2 terms, below and above 160 K where both the slopes and the intercepts in figure 2(b) change. For the crystals with $T_c = 65$ K, 40 K and 26.5 K, α_1 and α_2 were found from the intercepts at $T = 0$ and the slopes of the straight lines in figure 2(b), while the residual resistivity α_0 was then found by fitting the data in figure 2(a) to a second order polynomial in which α_1 and α_2 were fixed. The coefficients α are given in table 1. (A small correction for a measurement offset of $\sim 1\mu\Omega \cdot$cm below T_c has been included where appropriate). Here we focus on the values below 160 K, expecting them to be more closely related to superconductivity. The coefficient α_1 is presently of great interest because of the suggestion that the Planckian

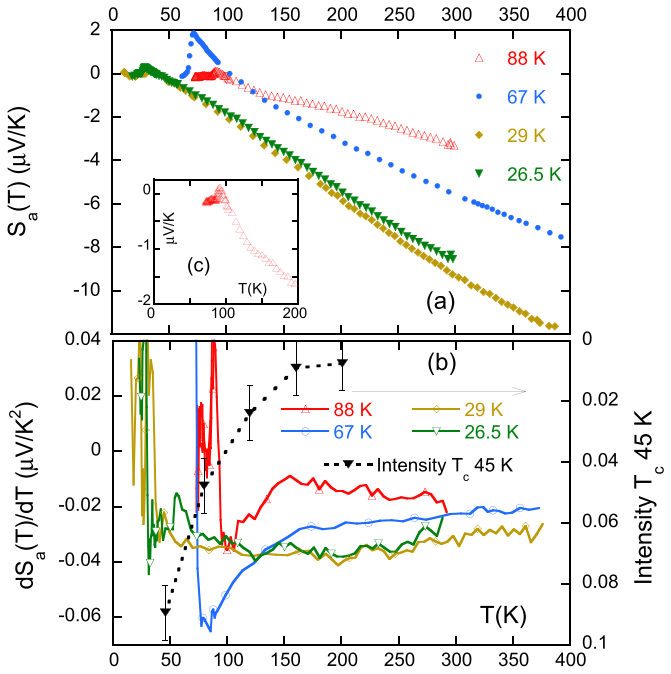

Figure 1. (a) In-plane thermoelectric power $S_a(T)$ for the same Tl2201 crystal with 4 different T_c values. $p = 0.192$, 0.220, 0.271 and 0.274 for $T_c = 88$ K, 67 K, 29 K and 26.5 K respectively determined from the same modified formula used in [1] that accounts for the Fermi surface area obtained from quantum oscillation studies [2] for $T_c \leqslant 26$ K. (b) Left-hand scale, corresponding derivative plots dS_a/dT, and right-hand scale RIXS intensity *vs* T for a crystal with $T_c = 45$ K from [3]. The CDW causes a downturn in dS_a/dT below 150 K, upturns at lower T are caused by the onset of superconductivity. Before forming the derivatives, $S_a(T)$ and T data were smoothed over 5 points, typically ± 10 K, 10 or 20 K above T_c and ± 4 K nearer T_c. This reduced the scatter without causing other changes. (c) Inset, expanded view for $T_c = 88$ K showing a clear anomaly at 145 K.

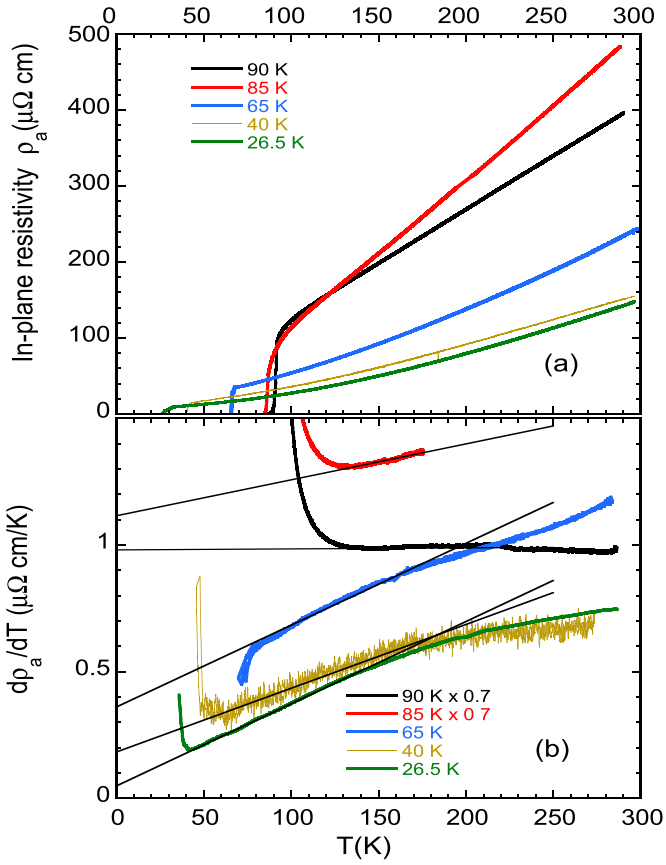

Figure 2. (a) In-plane resistivity data $\rho_a(T)$ for Tl2201 crystals from the same batch, taken from [1]. The crystal with $T_c = 85$ K is probably underdoped [1] and not considered further here. The p values for the other crystals are 0.183, 0.227, 0.256 and 0.274 for $T_c = 90$ K, 65 K, 40 K and 26.5 K respectively. (b) Corresponding derivative plots and straight lines expected when $\rho_a(T) = \alpha_0 + \alpha_1 T + \alpha_2 T^2$. Data above 175 K for $T_c = 85$ K were too noisy to give accurate derivatives. The straight lines show the results of least squares fits.

scattering rate $\hbar/\tau \approx k_B T$ [6] is the maximum allowed for any material [8], and that it is an important intrinsic property of superconducting cuprates [7] and many other correlated metals [8]. The Drude formula for the in-plane conductivity of an isotropic cylindrical Fermi surface, $\sigma = ne^2\tau/m^*$, which is a reasonable first approximation for Tl2201, shows that $\alpha_1 = 1\ \mu\Omega \cdot \mathrm{cm\,K^{-1}}$ corresponds to $\hbar/\tau \approx 3.3 k_B T$, if the carrier density $n = 1.3$ holes per unit cell and $m^* = 5.2 m_e$. Although this value of m^* has been measured by QO only for OD Tl2201 [2], specific heat data [9] show that it only varies weakly with p. So $\alpha_1 = 0.3\ \mu\Omega \cdot \mathrm{cm\,K^{-1}}$ in figure 2(b) corresponds to $\hbar/\tau = k_B T$. For crystals with $T_c < 50$ K, $\hbar/\tau$ falls below this value because, as found previously [16, 17], the size of the T^1 term falls linearly to zero as p approaches the edge of the superconducting dome. This could be an indication that the anomalous scattering becomes confined to certain parts of the Fermi surface, in contrast to the results for some other cuprates [7]. The value of α_0 for $T_c = 26.5$ K in table 1, gives $\hbar/(k_B\tau) = 19$ K and for a Fermi velocity $v_F \equiv \hbar k_F/m^* = 1.7 \times 10^7\ \mathrm{cm\,s^{-1}}$, a mean free path of 68 nm. Specific heat data for Tl2201 [9] show a large residual linear term which increases as p approaches the edge of the superconducting dome, as expected for a d-wave superconductor when $\hbar/(k_B\tau)$ becomes comparable with T_c.

Previously [16] the deviations from a straight line above 160 K for the three most overdoped crystals in figure 2(b). were interpreted in terms of a parallel conducting channel and the maximum resistivity of 1800 $\mu\Omega \cdot$cm obtained when the carrier mean free path is equal to the in-plane lattice spacing a. However they are still clearly visible for the two most overdoped crystals in figure 2(a) that have resistivities as low as 60 $\mu\Omega \cdot$cm at 160 K and as mentioned already for another crystal from a different preparation batch with $T_c = 17$ K. Therefore we have no clear interpretation of this effect. It is worth noting that α_2 is rather insensitive to p as also shown in [16]. At 160 K it corresponds to a T^2 term in the resistivity of 40 $\mu\Omega \cdot$cm and, making the same assumptions as before, a scattering rate $\hbar/\tau = k_B T$, the Planck condition [6]. This observation could have ramifications for interpretations of the T^1 term arising from the Planck condition. Perhaps $\hbar/\tau \geqslant k_B T$

Table 1. Values of α given by the straight lines below 160 K in figure 2(b) plus a constrained fit to the data in figure 2(a) (see text), i.e. $\rho(T) = \alpha_0 + \alpha_1 T + \alpha_2 T^2$. The carrier mean free path (mfp) is obtained from α_0. $T_c^{\rm TEP}$ values are from figure 1(a). S_0, S_1 and S_2 are from fits to equation (2), but cannot be determined independently (see text). The errors in α values are $\pm 10\%$ from geometrical uncertainties.

T_c (K)	α_0 ($\mu\Omega\cdot$cm)	α_1 ($\mu\Omega\cdot$cm K^{-1})	$\alpha_2 \times 1000$ ($\mu\Omega\cdot$cm) K^{-2})	mfp (nm)	$T_c^{\rm TEP}$ (K)	S_0/T (μV K^{-2})	S_1/T (μV K^{-2})	S_2/T (μV K^{-2})
90	(6.4 ± 0.4)	1.37	0.125	—	88	0.132	$-0.0115 \pm 6\%$	—
65	6.3	0.313	1.82	65	67	0.128	—	$-0.030 \pm 10\%$
40	6.9	0.17	1.34	60	—	—	—	—
26.5	6.0	0.053	1.6	68	26.5	0.016	—	$-0.033 \pm 3\%$

might cause the deviations from linearity in figure 2(b) above 160 K. Alternatively the deviations might be connected with the effect of lattice vibrations on electron–electron Umklapp scattering. Electron–electron scattering is rarely studied up to such high temperatures. It is known that the Debye–Waller factor, which reduces the intensity of x-ray diffraction lines, causes the energy gap of semiconductors such as Si to fall as T is increased. It is possible that Umklapp scattering between Brillouin zones is reduced by a similar T-dependent factor that becomes more significant as the amplitude of the lattice vibrations increases.

Data for all hole-doped cuprates clearly show that the curvature of in-plane $\rho(T)$ plots increases on the OD side. It is widely accepted that there is a crossover line on the $T-p$ phase diagram [18], which although ill-defined, increases linearly with p from zero for $p \geqslant 0.19$. It can be interpreted as a coherence temperature $T_{\rm coh}(p)$ for the charged carriers and when $T \lesssim T_{\rm coh}$ the T^2 term dominates. The results for $T \leqslant$ 160 K in figure 2(b) and table 1 are *qualitatively* consistent this is because α_1 falls with p while α_2 stays constant. For $T \geqslant$ 160 K this requires the slope of $d\rho_a/dT$ to become constant which is the case above 200 K for $T_c = 30$ K [16] and for data in [15] above 250 K for several T_c values between 0 and 80 K. It is puzzling that this does not hold for $T_c = 65$ K in figure 2(b) suggesting that more data are needed to clarify this point. We note that there can be complications from Cu ions on the Tl sites affecting p [14] as well as time dependent changes in T_c when a Tl2201 crystal is held at room temperature [19] that were also seen in our TEP data for $T_c = 26.5$ K after one month at room temperature after the first anneal.

2.3. Pair breaking vs 'Not-pairing'

There seems to be two possible ways of explaining the variation of α_1 and T_c with p, which we will refer to as scenarios A and B. The more standard one, scenario A, based on the usual d-wave form for the pairing interaction, $V_{kk'} \propto (\cos k_x - \cos k_y)(\cos k'_x - \cos k'_y)$, has been thoroughly analyzed and discussed in [10, 11] and related papers where the importance of small angle scattering was emphasized. Here T_c falls as p is increased because the pairing interaction falls [12, 13] and hence $(\hbar/\tau)/\Delta$ where Δ is the superconducting energy gap, is larger. The theory is very similar to that used to understand the effect of magnetic impurities in classical superconductors. Experimental evidence for the relation between T_c and $\rho_{\rm res}$ is summarized in [20] for both UD and OD cuprates. A second, less conventional one, scenario B, involves a different variation of the pairing interaction around the Fermi surface and is considered later. Scenario A could be referred to as 'pair-breaking' and B as 'not-pairing'. For our data set, the values of α_0 for the OD65, OD40 and OD26 crystals in table 1 are very close to that in [11] for their OD25 crystal measured using microwaves.

2.4. NG analysis

In standard transport theory, when there are two or more independent scattering mechanisms, for example electron-impurity and electron-phonon scattering, giving contributions ρ_0 and ρ_1 to the resistivity, the total resistivity $\rho = \rho_0 + \rho_1$, which is known as Matthiessen's rule (MR). For ordinary metallic alloys MR is a good first approximation although there are systematic deviations from MR that are well-documented [21]. There is considerable experimental evidence for Zn-doped YBCO and LSCO that MR applies to the T—independent impurity scattering and the T^1 scattering terms in the cuprates [22–24]. The equivalent way of calculating the TEP is via the NG [25] rule:

$$S_{\rm NG} = (\rho_0 S_0 + \rho_1 S_1 + \rho_2 S_2 + \cdots)\,/\,(\rho_0 + \rho_1 + \rho_2 + \cdots) \quad (2)$$

where S_0 and S_1 etc are the corresponding contributions to the TEP. If the electron diffusion TEP is dominant, and there are no small energy scales, these will be proportional to T, but with different signs and magnitudes governed by the energy dependence of the particular scattering mechanism. As shown in table 1 the T_c values in figure 1 are close enough to some of those in figure 2(a) so the coefficients α can be used directly to calculate the TEP via equation (2).

For $T_c \leqslant 67$ K the parameters S_0, S_1, and S_2, all assumed to be proportional to T, were found by fitting the TEP data in figure 1(a) to equation (2). The range of fit was very limited, to below 200 K because of deviations from equation (1) at higher T and for the two higher T_c values to above 150 K, because of the onset of the CDW. Partly as a result of this, only the parameter S_2 representing the contribution to the TEP from the T^2 resistivity term is well-defined, although the term S_0 from impurity scattering must be positive. This procedure did not work for T_c =90 K where it gave the very small value of α_2 shown in table 1 and a negative value for α_0. For this crystal we therefore set $\alpha_0 = 6.4 \pm 0.4$ $\mu\Omega\cdot$cm, the average for the other three T_c values, giving the values of S_1 and S_0 shown in table 1. For $T_c = 88$ K and 67 K S_0 must be at least 0.1μV K^{-2}

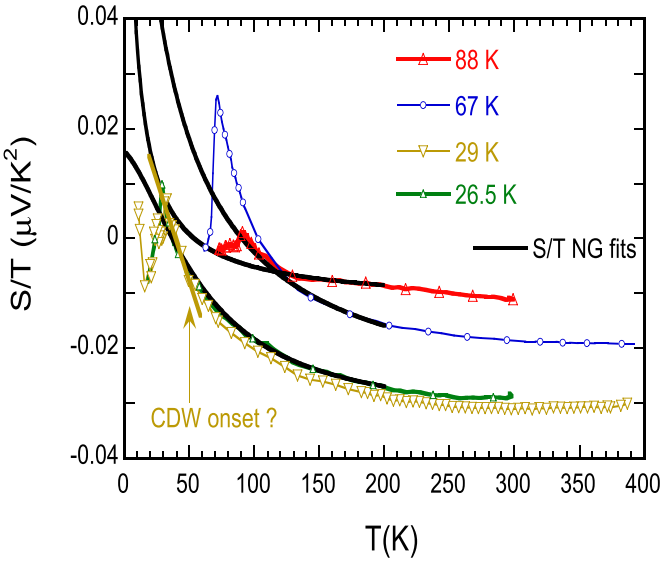

Figure 3. $S_a(T)/T$ *vs* T for $T_c = 88$ K, 67 K, 29 K and 26.5 K together with fits to equation (2) for T_c =88 K, 67 K and 26.5 K, solid lines, with parameters given in table 1.

which is unexpectedly large. In figure 3 it can be seen that the calculated S_{NG} curves for $T_c = 67$ K and 26.5 K, agree well with the data giving $S_2 = -0.033T\mu\text{V K}^{-1}$, of the same sign and approximately 3 times larger than S_1 for $T_c = 90$ K. We can therefore conclude that the energy dependence of the T^1 scattering term has the same sign as that of the T^2 term, which is generally attributed to electron–electron scattering, but is significantly smaller. Measurements in which the superconductivity is suppressed by a magnetic field and on crystals with different residual resistivity, possibly controlled by doping with in-plane impurities such as Zn, would provide a further test of this picture. The magnitude of S_2 is discussed below. Because of momentum conservation the electron–electron scattering contribution to $\rho(T)$ usually depends on Umklapp scattering processes which will generally tend to be stronger for larger energies. This implies that for electrons, the electron–electron scattering term S_2 will be positive and for holes it will be negative in agreement with experiment for Tl2201. Within this NG picture the changes in TEP below 160 K in figure 1(a) as p is increased are caused by the increase in the ratio $\alpha_2 T^2/\alpha_1 T$ with doping p and the fact that $-S_2$ is larger than $-S_1$.

2.5. Possible anisotropy around the Fermi surface, scenario B

In the previous sections it was assumed implicitly that the T^1 and T^2 scattering rates do not vary appreciably around the Fermi surface, so that their contributions to $\rho(T)$ can be added in the same way as for electron-phonon and electron-impurity scattering. This is only approximate because there is experimental evidence from angle-dependent magnetoresistance (ADMR) of the c-axis resistivity [26] that for crystals with T_c = 20 K, 17 K and 15 K, the anisotropy, (the parameter α in [26]) increases from 15% at 20 K to 40% at 110 K. Recently, new short-range CDW signals have been identified in RIXS studies of many cuprate families [27]. These are present for a wide range of p, including the 'strange metal' region, $p > 0.19$, that is relevant for Tl2201 although such short range signals have not yet been observed for Tl2201. They are short-ranged in real space, and therefore broader in reciprocal space and are visible to higher T than the CDWs that have reasonably well-defined, often incommensurate, wave vectors $\underline{Q}$. It has been argued that [28] that scattering from these short-range charge density fluctuations (CDF) are responsible for the T^1 term in $\rho(T)$ and because the CDF have a wide range of $\underline{Q}$ vectors they would indeed give isotropic scattering. So if CDF could be observed in Tl2201 crystals a good experimental test of this approach would be to compare their intensities with the size of the T^1 terms in $\rho(T)$ for different values of p.

Calculations by Rice *et al* [29] are more consistent with scenario B. These are based on the theory of Yang *et al* [30] and show that Umklapp scattering between hot spots gives rise to a T^1 scattering rate in a very limited region of $\underline{k}$-space and a corresponding T^1 term in $\rho(T)$. They are not based on the usual Boltzmann transport equation. Somewhat paradoxically, in an earlier paper using the variational principle [31] to solve the Boltzmann equation, Hlubina and Rice [32] showed that the T^2 term will dominate, although of course at low enough T any non-zero T^1 term must become larger than a term going as T^2. In this scenario $1/\tau$ at or near the hot spots is likely to be close to the Planck value because for $p \simeq 0.19$ where any T^2 term is very small, as shown for example in table 1, $1/\tau$ is somewhat larger than the Planck value. It may be possible to distinguish between scenarios A and B by measuring the resistivity and London penetration depth on several crystals with similar T_c values. Scenario B provides a more direct link between the T^1 term and the superfluid density, emphasized recently in [17], than scenario A. However unlike scenario A it would not necessarily account for MR, the NG rule or the ADMR results. One possible test would be to see if either scenario can account for the 'vertical scaling' of the electronic specific heat [33] in applied magnetic fields.

2.6. Comparison with the TEP of other correlated electron materials

The low T TEP of many correlated electron materials, including some where the T^2 term in $\rho(T)$ is dominant, has been shown [34] to obey the following simple empirical formula:

$$\frac{S}{T} = \frac{\gamma q}{N_{\text{AV}} e}. \tag{3}$$

Here γ is the Sommerfeld coefficient, N_{AV} Avogadro's number and e the magnitude of the electronic charge. The Faraday number $N_{\text{AV}}e = 9.6 \times 10^4$ Coulombs/mole. For the simple case of free electron dispersion and 1 electron per formula unit, $q = -1$ so taking $\gamma = 0.6$ mJ $(\text{gm} \cdot \text{at})^{-1}\text{K}^{-2}$ [9] gives $S = -13$ $\mu\text{V K}^{-1}$ at 160 K, the end of the linear regions in figure 2(b). This will be reduced by a factor $1 + p \simeq 1.3$ by the larger carrier concentration and by a factor 2/3 for a constant carrier mean free path [34] giving -6.7 $\mu\text{V K}^{-1}$ at 160 K. The value of $-S_2 = 0.033T\mu\text{V K}^{-1}$ in table 1 gives a TEP of -5.3 $\mu\text{V K}^{-1}$ at 160 K. So the T^2 electron–electron scattering

term in our TEP data for Tl2201 crystals agrees well with findings [34] for many other correlated electron materials, while the contribution from the T^1 term is approximately a factor 3 smaller.

3. Summary

We have argued that the presence of CDWs can be seen in the in-plane TEP of Tl2201 crystals and in earlier data [5] for polycrystalline samples where the measured TEP is very similar to $S_a(T)$ for similar values of p. The NG rule seems to provide an adequate description of the TEP contributions arising from the T^1 and T^2 terms in the in-plane electrical resistivity. The magnitude of the TEP contribution from the T^2 term agrees with that for other correlated electron conductors [34] while the contribution from the T^1 term is $\sim$3 times smaller. If the T^1 term were truly anomalous one might perhaps have expected a larger difference. Within a simple cylindrical Fermi surface approximation, taking into account the known value of m^*, the T^1 terms for the crystals with T_c of 40 K and 26.5 K correspond to scattering rates $1/\tau$ that are significantly smaller than the Planckian value $k_BT/\hbar$, possibly indicating that τ is anisotropic. A strongly anisotropic scattering rate could provide a direct way of understanding the apparent correlation between the magnitude of the T^1 term and the superfluid density emphasized recently [17], namely only those carriers with a T^1 scattering rate would be paired. But there could be difficulties in accounting for MR, the NG rule and the ADMR work which suggests a small anisotropy at low T [26]. Also an extremely strong variation in $V_{kk'}$ might not be consistent with d-wave behavior. Somewhat unexpectedly, near 160 K, the T^2 term corresponds to a scattering rate $1/\tau \gtrsim k_BT/\hbar$ for all values of the hole concentration.

Data availability statement

All data that support the findings of this study are included within the article (and any supplementary files).

Acknowledgments

This work was funded by the EPSRC (U.K.) Grant Number EP/K016709/1. We are grateful to Prof. N E Hussey for helpful comments on the first draft of the manuscript.

Appendix

A.1. Method used for TEP

The basic method used for the TEP is similar to that originally used for sintered polycrystalline bars in [5], but because of the small size of the crystals, and the fact that thicker crystals or thin films on a crystalline substrate have high thermal conductance, Au reference wires and Chromel wires forming two differential thermocouples are attached to Au pads on the ends of the crystal as shown in the photograph in figure A1. These

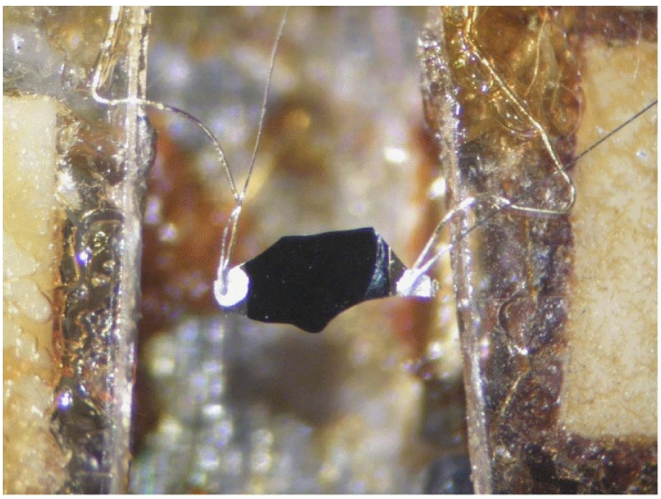

Figure A1. Photo of the 1.5 mm long Tl2201 crystal used for TEP measurements. 50 μm diameter Au wires and 25 μm diameter Chromel wires are spot-welded together to form differential thermocouples that are attached to Au pads on the crystal with DuPont 4929 N silver paint. The Au wires are heat sunk to sapphire plates with General Electric GE-7031 low temperature varnish.

wires extend for a few centimeters before being soldered to Cu wires heat sunk to a high thermal conductivity Cu block. A temperature difference ($\Delta T \lesssim 1$ K) is produced by alternately heating two sapphire blocks to which the thermocouple wires are attached with General Electric GE-7031 low temperature varnish and the Seebeck coefficient of the sample $S_{\rm sample}$ is given by eliminating ΔT from the equations:

$$V_{\rm Au-Au} = (S_{\rm sample} - S_{\rm Au})\,\Delta T \tag{A.1}$$

$$V_{\rm Ch-Ch} = (S_{\rm sample} - S_{\rm Ch})\,\Delta T \tag{A.2}$$

Here the voltages across the Au wires, $V_{\rm Au-Au}$ and the Chromel wires, $V_{\rm Ch-Ch}$ are measured using a Keithley Instruments digital nanovoltmeter and a home-built nanovolt amplifier respectively, and their ratio obtained by making a least squares linear fit to a plot of $V_{\rm Ch-Ch}$ *vs* $V_{\rm Au-Au}$ for $\pm\Delta T$ and two points with $\Delta T = 0$. $S_{\rm Ch}$ is the Seebeck coefficient of Chromel taken from published standards and shown in figure A2. The same reel of 50 μm diameter Au wire was always used and $S_{\rm Au}$, also shown in figure A2 was obtained by measuring a strip of pure Pb which has a low TEP [35].

In the past further checks have been made by measuring a superconducting cuprate, Bi2212 with $T_c \simeq 90$ K, and a piece of 127 μm diameter phosphor bronze alloy wire purchased from Lake Shore Cryotronics which has a conveniently low TEP. In the present work a piece of the same wire was measured again and compared with earlier data, as shown in figures A3(a) and (b). Small changes in the TEP of Au can be induced by bending (cold working) the wire which will change the phonon drag component and the electron diffusion component from any Fe impurities. Measuring the phosphor bronze wire is a convenient method of correcting for such changes. Figure A3(c) shows the TEP data from figure 1(a)

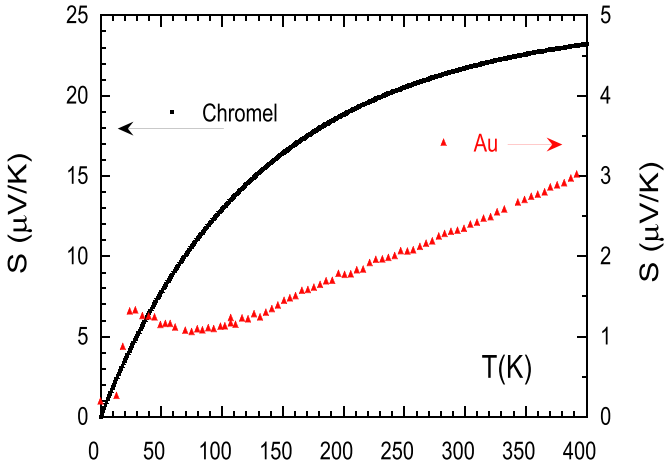

Figure A2. Thermopower of Chromel and Au wires used in the present work.

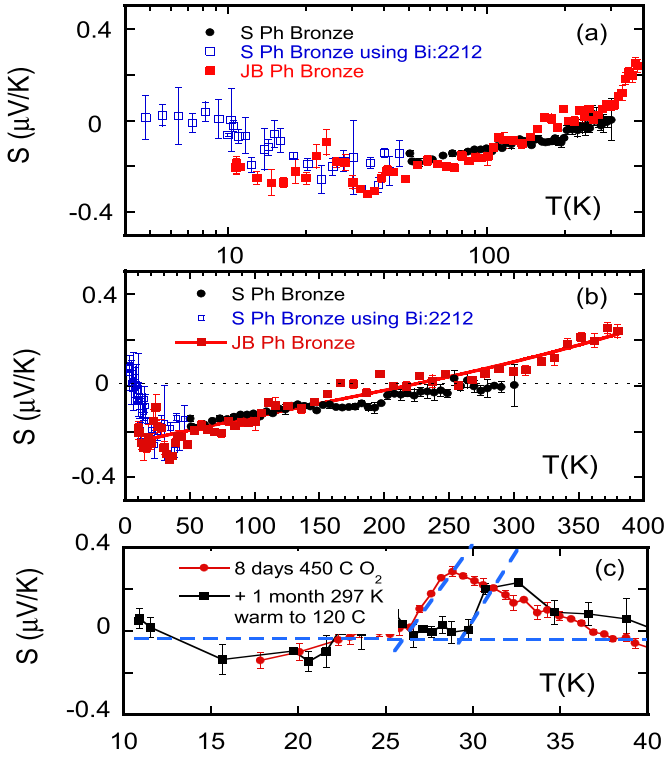

Figure A3. (a) and (b) TEP of Lake Shore Cryotronics phosphor bronze alloy wire on logarithmic and linear temperature scales respectively. The most recent data labeled JB Ph Bronze is compared with earlier measurements, including one data set where the superconducting Bi2212 sample had zero TEP below 85 K. (c) Low T data for the Tl2201 crystal after making a small correction of $\sim$0.1 μV K^{-1}, given by the data in (a). The dashed lines show how T_c values of 26 K and 29 K are determined.

after making a small correction of $\sim$0.1 μV K^{-1} corresponding to the difference in the TEP of the phosphor bronze wire at low T in earlier and more recent measurements shown in figure A3(a). It can be seen that T_c rises from 26 ± 1 to 29 ± 1 K after one month at room temperature after the first anneal.

ORCID iD

J R Cooper https://orcid.org/0000-0003-4279-1667

References

[1] Putzke C *et al* 2021 Reduced Hall carrier density in the overdoped strange metal regime of cuprate superconductors *Nat. Phys.* **17** 826–31

[2] Rourke P M C, Bangura A F, Benseman T M, Matusiak M, Cooper J R, Carrington A and Hussey N E 2010 A detailed de Haas-van Alphen effect study of the overdoped cuprate $Tl_2Ba_2CuO_{6+\delta}$ *New J. Phys.* **12** 105009

[3] Tam C C, Zhu M, Ayres J, Kummer K, Yakhou-Harris F, Cooper J R, Carrington A and Hayden S M 2022 Charge density waves and Fermi surface reconstruction in the clean overdoped cuprate superconductor $Tl_2Ba_2CuO_{6+\delta}$ *Nat. Commun.* **13** 570

[4] Hussey N E 2023 private communication

[5] Obertelli S D, Cooper J R and Tallon J L 1992 Systematics in the thermoelectric power of high-T_c oxides *Phys. Rev.* B **46** 14928–3

[6] Zaanen J 2004 Why the temperature is high *Nature* **430** 512–3

[7] Legros A *et al* 2019 Universal T-linear resistivity and Planckian dissipation in overdoped cuprates *Nat. Phys.* **15** 142–7

[8] Hartnoll S A and Mackenzie A P 2022 Colloquium: Planckian dissipation in metals *Rev. Mod. Phys.* **94** 041002

[9] Wade J M, Loram J W, Mirza K A, Cooper J R and Tallon J L 1994 Electronic specific heat of $Tl_2Ba_2CuO_{6+\delta}$ from 2 K to 300 K for $0 \leqslant \delta \leqslant 0.1$ *J. Supercond.* **7** 261–4

[10] Lee-Hone N R, Özdemi H U, Mishra V, Broun D M and Hirschfeld P J 2020 Low energy phenomenology of the overdoped cuprates: viability of the Landau-BCS paradigm *Phys. Rev. Res.* **2** 013228

[11] Deepwell D, Peets D C, Truncik C J S, Murphy N C, Kennett M P, Huttema W A, Liang R, Bonn D A, Hardy W N and Broun D M 2013 Microwave conductivity and superfluid density in strongly overdoped $Tl_2Ba_2CuO_{6+\delta}$ *Phys. Rev.* B **88** 214509

[12] Storey J G, Tallon J L and Williams G V M 2007 Saddle-point van Hove singularity and the phase diagram of high-T_c cuprates *Phys. Rev.* B **76** 174522

[13] Huang E W, Scalapino D J, Maier T A, Moritz B and Devereaux T P 2017 Decrease of d-wave pairing strength in spite of the persistence of magnetic excitations in the Hubbard model *Phys. Rev.* B **96** 0205030(R)

[14] Cooper J R, Baglo J C, Putzke C and Carrington A 2023 Annealing of Tl2201 crystals *Supercond. Sci. Technol. Suppl. Inf.*

[15] Tyler A W 1997 An investigation into the magnetotransport properties of layered superconducting perovskites *PhD Thesis* University of Cambridge

[16] Hussey N E, Gordon-Moys H, Kokalj J and McKenzie R H 2013 Generic strange-metal behaviour of overdoped cuprates *J. Phys.: Conf. Ser.* **449** 012004

[17] Culo M, Duffy C, Ayres J, Berben M, Hsu Y T, Hinlopen R D H, Bernáth B and Hussey N E 2021 Possible superconductivity from incoherent carriers in overdoped cuprates *SciPost Phys.* **11** 012

[18] Hussey N E 2008 Phenomenology of the normal state in-plane transport properties of high-Tc cuprates *J. Phys.: Condens. Matter* **20** 123201

[19] Mackenzie A P, Julian S R, Sinclsir D C and Lin C T 1996 Normal-state magnetotransport in superconducting $Tl_2Ba_2CuO_{6+\delta}$ to millikelvin temperatures *Phys. Rev.* B **53** 5848
[20] Rullier-Albenque F, Vieillefond P A, Alloul H, Tyler A W, Lejay P and Marucco J F 2000 universal T_c depression by irradiation defects in underdoped and overdoped cuprates? *Europhys. Lett.* **50** 81
[21] Cimberle M R, Bobel G and Rizzuto C 1974 Deviations from Matthiessen's rule at low temperatures: an experimental comparison between various metallic alloy systems *Adv. Phys.* **23** 639–71
[22] Cooper J R, Obertelli S D, Freeman P A, Zheng D N, Loram J W and Liang W Y 1991 Evidence for Matthiessen's rule in the normal state resistivity of zinc doped yttrium barium copper oxide *Supercond. Sci. Technol.* **4** S277–9
[23] Walker D J C, Mackenzie A P and Cooper J R 1995 Transport properties of zinc-doped $YBa_2Cu_3O_{7-\delta}$ thin films *Phys. Rev.* B **51** 15653–6
[24] Fukuzumi Y, Mizuhashi K, Takenaka K and Uchida S 1996 Universal superconductor-insulator transition and T_c depression in Zn-substituted high- T_c cuprates in the underdoped regime *Phys. Rev. Lett.* **76** 684–7
[25] MacDonald D K C 1962 *Thermoelectricity: An Introduction to the Principles* (Wiley)
[26] French M M J, Analytis J G, Carrington A, Balicas L and Hussey N E 2009 Tracking anisotropic scattering in overdoped $Tl_2Ba_2CuO_{6+\delta}$ above 100 K *New J. Phys.* **11** 055057
[27] Arpaia R and Ghiringhelli G 2021 Charge order at high temperature in cuprate superconductors *J. Phys. Soc. Japan* **90** 111005
[28] Seibold G, Arpaia R, Peng Y Y, Fumagalli R, Braicovich L, Di Castro C, Grilli M, Ghiringhelli G and Caprara S 2021 Strange metal behaviour from charge density fluctuations in cuprates *Commun. Phys.* **4** 7
[29] Rice T M, Robinson N J and Tsvelik A M 2017 Umklapp scattering as the origin of T-linear resistivity in the normal state of high-T_c cuprate superconductors *Phys. Rev.* B **96** 220502(R)
[30] Yang K Y, Rice T M and Zhang F C 2006 Phenomenological theory of the pseudogap state *Phys. Rev.* B **73** 174501
[31] Ziman J M 1960 *Electrons and Phonons: The Theory of Transport Phenomena in Solids* (Oxford University Press) ch 7
[32] Hlubina R and Rice T M 1995 Resistivity as a function of temperature for models with hot spots on the Fermi surface *Phys. Rev.* B **51** 9253
[33] Radcliffe J W, Loram J W, Wade J M, Wltschek G and Tallon J L 1996 Electronic specific heat of overdoped $Tl_2Ba_2CuO_{6+\delta}$ in a magnetic field *J. Low Temp. Phys.* **105** 903
[34] Behnia K, Jaccard D and Flouquet J 2004 On the thermoelectricity of correlated electrons in the zero-temperature limit *J. Phys.: Condens. Matter* **16** 5187–98
[35] Christian J W, Jan J P, Pearson W B, Templeton I M and Mott N F 1958 Thermo-electricity at low temperatures. VI. A redetermination of the absolute scale of thermo-electric power of lead *Proc. R. Soc.* A **245** 213–21